



# *In vitro* Degradation Studies on Mg-Zn-CeO<sub>2</sub> Composites for Biodegradable Implant Applications

Nagoju Manikanta Sarath Kumar <sup>1,2</sup>, Gamini Suresh <sup>3</sup>, Ravikumar Dumpala <sup>4</sup>, Ratna Sunil Bradagunta <sup>5,\*</sup>

<sup>1</sup> Department of Mechanical Engineering, Vignan's Foundation for Science, Technology & Research, Vadlamudi 522213, India; sarath.vlits@gmail.com (N.M.K.S.K.);

<sup>2</sup> Department of Mechanical Engineering, Vignan's LARA Institute of Technology & Science, Vadlamudi 522213, India;

<sup>3</sup> Department of Mechanical Engineering, Vignan's Foundation for Science, Technology & Research, Vadlamudi 522213, India; drgs.mech@gmail.com (G.S.);

<sup>4</sup> Department of Mechanical Engineering, Visvesvaraya National Institute of Technology, Nagpur 440010, India; ravikumardumpala@mec.vnit.ac.in (R. K.D.);

<sup>5</sup> Department of Mechanical Engineering, Bapatla Engineering College, Bapatla 522101, India; bratnasunil@gmail.com (B. R. S.);

\* Correspondence: bratnasunil@gmail.com (B.R.S.);

Scopus Author ID 35410353400

Received: 13.06.2023; Accepted: 13.11.2023; Published: 20.07.2024

**Abstract:** The development of magnesium (Mg) based biodegradable implants for temporary applications in biomedical engineering is a prospective research area. Recently, several new Mg alloys and composites were developed, and their efficacy as implant materials to manufacture temporary implants was assessed. Developing composites facilitates taking advantage of the diversified properties from the constituting phases in a single material. Hence, in the present study, cerium dioxide (CeO<sub>2</sub>) particles were added to Mg-1% Zn alloy with different fractions of the reinforcement through a stir casting route to experimentally investigate the *in vitro* degradation behavior in simulated environmental conditions. No impurities or formation of intermetallics were identified from the X-ray diffraction (XRD) studies and microstructural investigations. The presence of more CeO<sub>2</sub> led to grain refinement (from 165 ± 12.3µm to 105 ± 7.1µm). The phases on the surface of the samples from the *in vitro* immersion study were assessed by XRD and scanning electron microscopy and observed that the composite with higher CeO<sub>2</sub> has more mineral phases compared with the base alloy and the other composites. From the weight loss measurements, lower weight loss was observed for the composite with 2% CeO<sub>2</sub>. With the increased content of CeO<sub>2</sub> up to 4%, the weight loss was marginally increased, which is attributed to the combined effect of increased galvanic corrosion and decreased degradation due to the deposited mineral phases. The results suggest the potential of adding CeO<sub>2</sub> to Mg-1%Zn alloy to tailor the degradation for temporary implant applications.

**Keywords:** magnesium; zinc; cerium dioxide; biomaterials; implants; degradation.

© 2024 by the authors. This article is an open-access article distributed under the terms and conditions of the Creative Commons Attribution (CC BY) license (<https://creativecommons.org/licenses/by/4.0/>).

## 1. Introduction

Developing new magnesium (Mg) alloys and composites grabbed the attention of several research groups in biomedical engineering for the past two decades as potential candidates for manufacturing temporary implants [1]. Mg exhibits excellent biocompatibility and non-toxicity when used as a biomaterial. However, rapid degradation is an issue with Mg implants, which has been the field of interest of materials scientists for the past two decades to develop new technologies to counter the limitations of Mg implants [2]. In this connection, <https://biointerfaceresearch.com/>

several Mg alloys with principal alloying elements, such as Zn, Al, Zr, Sr, Ca, Si, Mn, Nd, Y, La, Gd, etc., have been widely studied for implant applications [3, 4]. On the other hand, adding biocompatible ceramic phases into a suitable Mg alloy brings additional advantages in promoting the life span of the implant to achieve wide acceptability by the local host for longer durations in the physiological environment [5]. Hydroxyapatite (HA), tricalcium phosphate (TCP), MgO, CNTs, Al<sub>2</sub>O<sub>3</sub>, SiO<sub>2</sub>, and TiO<sub>2</sub> are a few examples of reinforcing phases used to develop Mg composites for bio-implant applications [6-10]. Zn is an essential micronutrient for regulating metabolic activities in the human system. Zn also exhibits a non-toxic nature when used in lower concentrations and helps to promote cell growth [11]. Zn dissolves in Mg at room temperature to form solid solution grains. However, the solubility of Zn is limited to less than 1% in the binary alloy of Mg and Zn [12]. Excess amounts of Zn in Mg more than the solubility limit lead to hard and brittle intermetallics [13]. Hence, limiting the content of Zn to lower values in Mg-Zn binary alloys for medical implant applications is suggested.

Recently, interest in cerium oxide (CeO<sub>2</sub>) particles has been gradually growing due to their wide usage in several medical applications, including drug delivery, regenerative medicine, bio-coatings, biosensors, tissue engineering, etc. [14-16]. It has been widely reported that CeO<sub>2</sub> can help promote cell growth and proliferation and quick wound healing [17-19]. From the works of Kalyanaraman et al. [20], the toxicity of CeO<sub>2</sub> is negligible, similar to many ceramic-compatible materials, and as a biomaterial, CeO<sub>2</sub> has more potential to be used to develop new material systems. It was observed that CeO<sub>2</sub> has been incorporated into different polymers, and nanocomposites have been developed to improve their mechanical and thermal properties [21]. Furthermore, as a coating material, several surfaces were coated with CeO<sub>2</sub>, and several surfaces were coated with CeO<sub>2</sub>, and enhanced surface properties have been achieved [22]. However, the literature on developing biomedical Mg composites dispersed with CeO<sub>2</sub> is insufficient. In particular, developing Mg-1%Zn composites dispersed with CeO<sub>2</sub> is lacking. Hence, in the current work, Mg-1%Zn alloy has been selected as the base alloy, and composites were developed by dispersing different fractions of CeO<sub>2</sub> to study the effect of CeO<sub>2</sub> presence on the *in vitro* degradation by conducting immersion studies.

## 2. Materials and Methods

Pure Mg billet (99.9%) was purchased from Exclusive Magnesium, India, and pure Zn powder was procured from Quality Traders, Guntur, India. Nano-CeO<sub>2</sub> powder (100nm) was obtained from Nano-Wings, Khammam, India. Initially, Mg-1% Zn master alloy was produced through the stir casting route. Then, Mg-1% Zn was used as the matrix material, and the composites were designed by selecting 1%, 2%, and 4% CeO<sub>2</sub> reinforcements. Appropriate weights were measured, added in a graphite crucible in the stir casting furnace, and slowly heated to 800°C in the protective environment. Then, the liquid mix of the composite was stirred with the help of a steel propeller at 200 rpm for 10 minutes to ensure the appropriate mixing of the reinforcements. The composites were named composite 1, composite 2, and composite 4 for the samples having 1%, 2%, and 4% CeO<sub>2</sub>, respectively. Microstructural studies were done by recording the microstructures by polishing and etching the samples. The samples were subjected to X-ray diffraction analysis (XRD, Bruker, USA) between 20° to 80° with a scanning speed of 0.1°/s. All the peaks of the XRD patterns were analyzed and indexed by comparing them to the standard data.

The degradation behavior of the samples was assessed by *in vitro* immersion studies using simulated body fluids (SBF). Immersion studies in SBF provide the typical behavior of the samples in the physiological environment. Assessing the material's response in SBF can be useful for understanding the material's performance when exposed to a real-time bio-environment. Lab-grade chemical reagents (KCl, NaCl, NaHCO<sub>3</sub>, CaCl<sub>2</sub>, K<sub>2</sub>HPO<sub>4</sub>, MgCl<sub>2</sub>·6H<sub>2</sub>O, and Na<sub>2</sub>SO<sub>4</sub>) were procured from Merck, India to prepare the SBF. The methodology to prepare the SBF and the concentration of the constituting ions are explained elsewhere [23, 24]. All the samples of size 10 x 10 x 1mm<sup>3</sup> were prepared for the immersion studies. Initially, all the samples prepared for immersion studies were subjected to fine polishing to remove the effect of surface roughness and thoroughly cleaned with distilled water. Then, the samples were immersed in 50ml SBF in a container maintained at a constant temperature of 37°C. The sample weights were recorded before being immersed in the SBF for 24h, 48h, and 72h. The change in the pH of the solution was measured every 12h to assess the change in the solution ion concentration. After immersion studies, the samples were collected and subjected to morphological studies by scanning electron microscope (SEM, TESCON, Czech Republic). The surface deposits and corrosion products' elements were assessed by energy-dispersive X-ray spectroscopy (EDS). The phase analysis of the sample surface was done by XRD. After immersion studies, the samples were placed in the boiling solution of CrO<sub>3</sub> for 30 minutes to dissolve the corrosion products. The weight of the samples was recorded, and the average % of the weight loss of the samples was calculated and compared.

### 3. Results and Discussion

The microstructures of the samples are presented in Figure 1. It is clear from the images that the addition of CeO<sub>2</sub> has a marginal effect on reducing the average grain size of the composites compared with Mg1Zn. Compared with the base alloy (165 ± 12.3µm), composites were measured with smaller grain sizes. With the increased content of the reinforcement, the grain size in the composites was further measured as decreased. Compared with composite 1 (122 ± 5.8µm) grain size, composite 2 (108 ± 6.3µm) and composite 4 (105 ± 7.1µm) have smaller grain sizes. The presence of heterogeneous phases in the liquid indeed leads to the development of more nuclei during the solidification process of metals and alloys. During the solidification of the Mg1Zn alloy, the added CeO<sub>2</sub> acted as nuclei and increased the number of centers that grew during crystallization. Therefore, more grains are expected to be obtained, which will result in reduced grain size. The presence of reinforcement can be seen as black particles in the microstructures of the composites in Figure 1. More such particles can be visible with the increased content of the reinforcement. The XRD analysis of the samples confirms the phases present in the composites (Figure 2). All the peaks were identified and confirmed as solid solution α-Mg. A higher fraction of CeO<sub>2</sub> was detected in the composites, as reflected by the appearance of a few peaks with smaller intensities (composites 4). No new peaks corresponding to any impurity or development of new phases were observed.

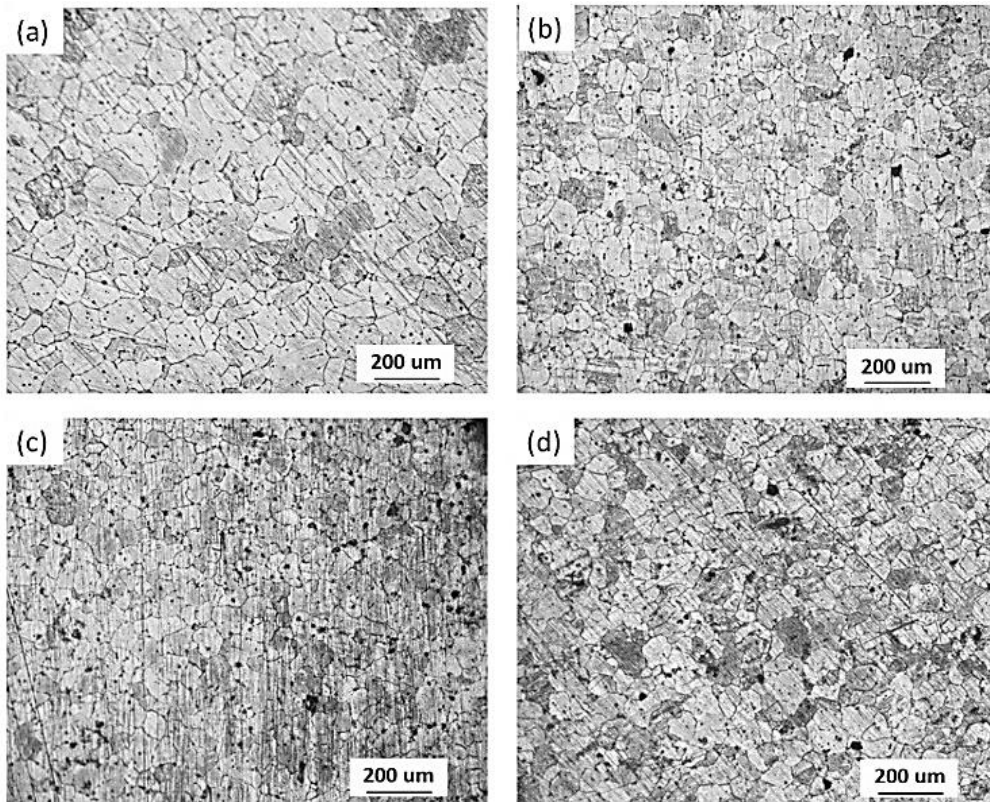


**Figure 1.** Microstructures of the samples: (a) Mg1Zn; (b) composite 1; (c) composite 2; (d) composite 4.

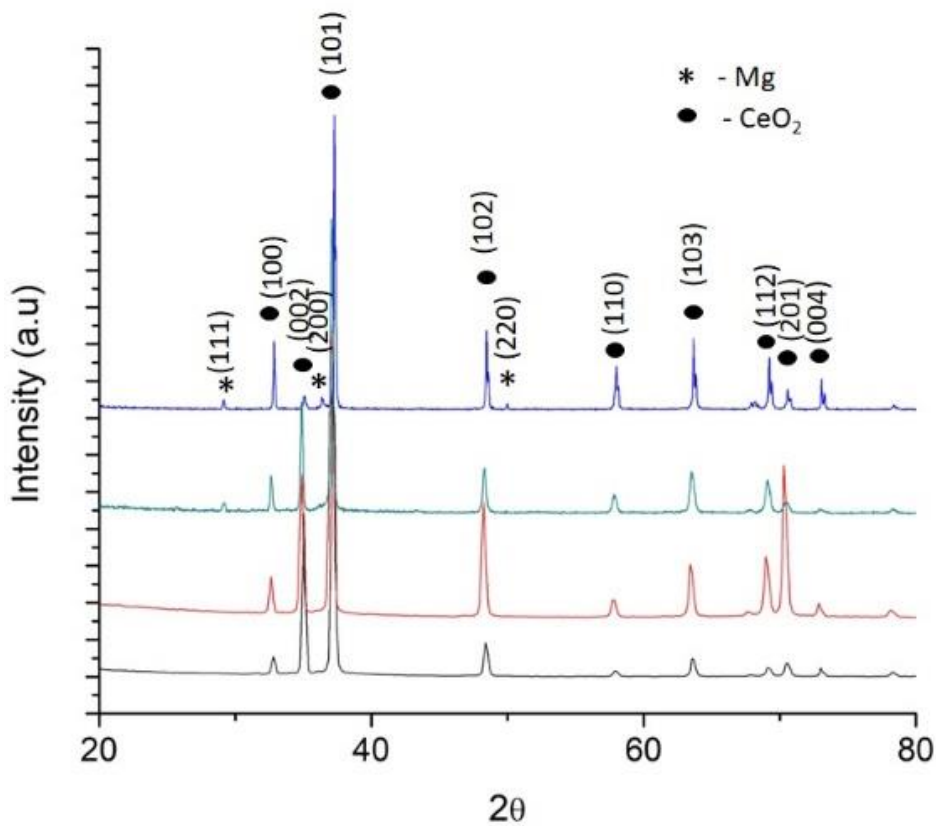


**Figure 2.** XRD patterns of the samples.

The surface morphologies of the samples subjected to 72 immersion are shown in Figure 3, and the corresponding XRD patterns are shown in Figure 4. The presence of  $\alpha$ -Mg, CeO<sub>2</sub>, and magnesium hydroxide phases has been identified from XRD results. The surface

<https://biointerfaceresearch.com/>

morphologies of the immersed samples clearly show several corrosion products (Figure 3), and the EDS analysis also confirms the elements of the phases on the surfaces. The appearance of Mg and O elements in the EDS spectra is due to the development of a magnesium hydroxide layer on the sample due to corrosion in SBF. The presence of chlorine (Cl) indicates the formation of magnesium chloride. Furthermore, Ca and P elements were also observed in the EDS spectra, indicating the development of Ca-based apatite on the surface from the SBF solution. For the Mg1Zn sample, globular structures with needle-like morphology appeared.

Figure 5 shows a magnified image of the typical morphology of the surface of Mg1Zn sample. From the elemental composition (Figure 3(b)), the presence of more Cl can be observed compared with the composites. Usually, in the degradation process of Mg, the corrosion product of magnesium hydroxide is formed due to electrochemical reactions in an aqueous environment. The corrosion product (magnesium hydroxide) further protects the Mg substrate, reducing degradation [25, 26]. However, magnesium hydroxide is unstable in the presence of chloride ions, leading to the formation of magnesium chloride salt, which appears as needle-like structures, as observed in the present study.

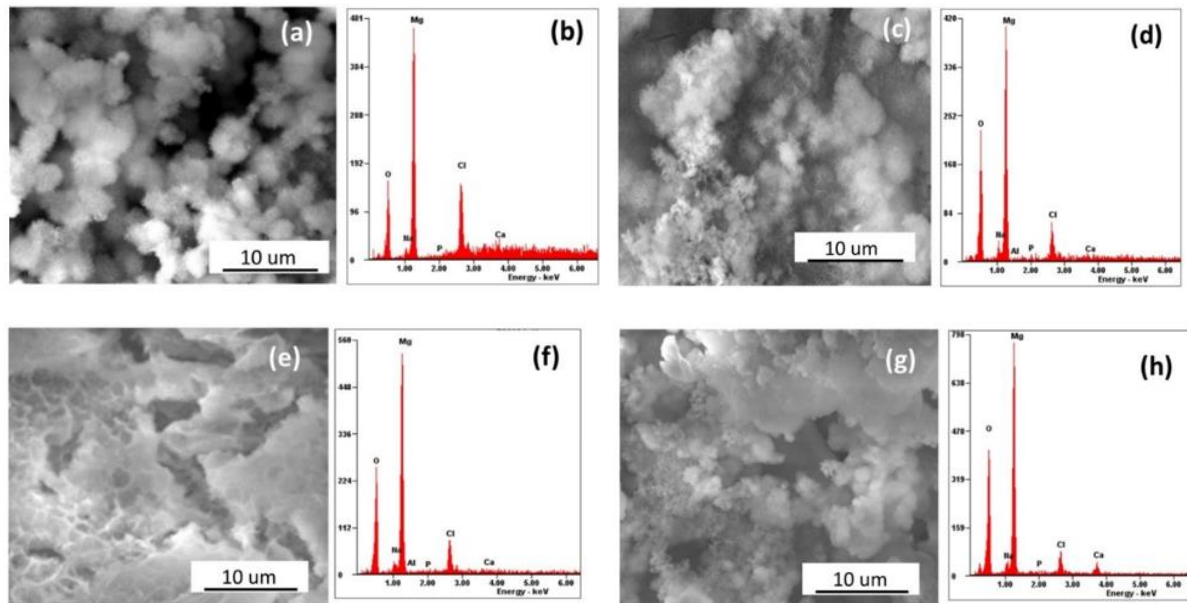


**Figure 3.** Surface morphologies and the corresponding EDS analysis of the samples after 72 h of immersion in SBF: (a) Mg1Zn; (b) EDS analysis of Mg1Zn; (c) composite 1; (d) EDS analysis of composite 1; (e) composite 2; (f) EDS analysis of composite 2; (g) composite 4; (h) EDS analysis of composite 4.

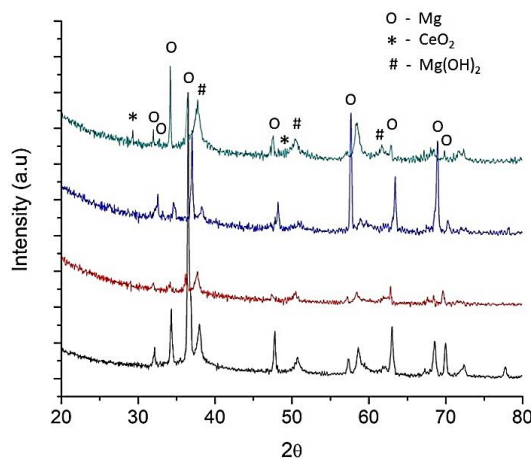


**Figure 4.** XRD patterns of the samples after 72 h of immersion in SBF.

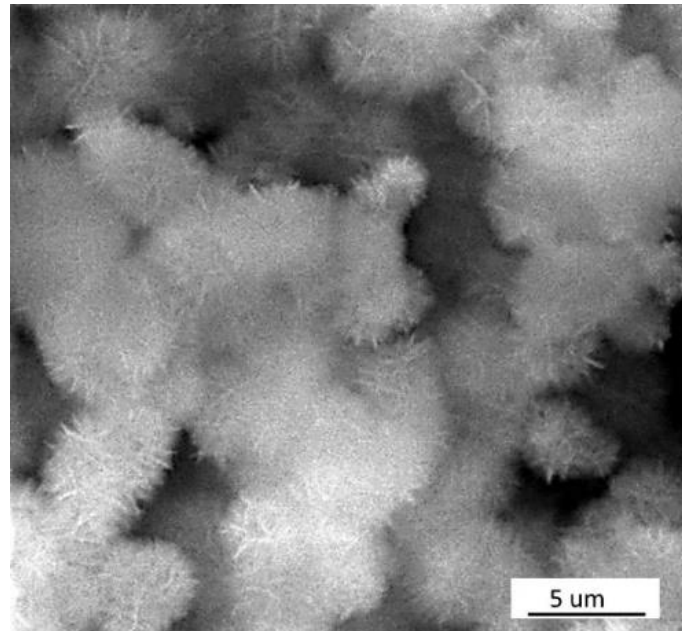


**Figure 5.** Surface corrosion product morphology on Mg1Zn sample after 72 h of *in vitro* immersion study.

The appearance of more magnesium chloride indicates the magnesium hydroxide's poor stability on the Mg substrate. This phenomenon makes Mg more vulnerable to the corroding environment in the presence of chloride ions. This is similar to the earlier reported works in which it was demonstrated that the appearance of more magnesium chloride on Mg substrate indicates higher degradation of Mg substrate [27]. On the other hand, the surface morphologies of the composites were different compared with base alloy (Figure 3 (c), (e), and (g)). The presence of more Ca and P can be seen with decreased Cl content on the composites compared with the Mg1Zn sample (Figure 3(d), (f), and (h)). This observation suggests the formation of magnesium chloride is lower, and deposition of Ca/P mineral from the SBF is higher on the composites compared with the base alloy. Since human body fluids contain chloride ions abundantly, degradation of Mg is rapid and uncontrolled when exposed to the body fluids. Interestingly, composites have shown the presence of lower Cl from the EDS analysis, which suggests the stability of the magnesium hydroxide layer is higher, which increases the life span of the Mg implant in the aggressive bio-environment. With the increased CeO<sub>2</sub> content, the appearance of Ca and P also increased, indicating increased mineral deposition from the SBF. Being a ceramic phase, the presence of more CeO<sub>2</sub> accelerated the mineral deposition from the SBF. In addition to stabilizing the magnesium hydroxide layer, adding CeO<sub>2</sub> also promotes biomineralization, a process by which mineral phases are deposited from the host environment on the implant can be accelerated. Improving biomineralization helps to increase the protection of the surface of the Mg implant, as demonstrated by the earlier reported works [28-30]. Therefore, in the present work, a stabilized magnesium hydroxide layer with more Ca-based mineral phases deposition on the composites has been observed, promising to enhance the performance of Mg1Zn alloy as a potential biomaterial.

Figure 6 compares the pH values of the SBF throughout the immersion test. In the initial hours, a rapid increment in the pH was noticed for the base alloy and the composites. After 12 hours of immersion, the pH values reached more than 9, and then after 24 hours of immersion, they gradually reached up to 10. This observation indicates the change in the ion concentration in the SBF during the initial hours of the degradation process. Therefore, the change in the local pH by releasing hydrogen gas is an important observation well understood in the literature

[31, 32]. However, in the real-time bio-environment, due to the dynamic nature of the ever-changing ion concentration, this issue is less of a concern. Among all the samples, 2% and 4% composites were observed with marginally lower pH values during the first 24h of immersion, and all the samples showed insignificant differences after 48h and 72h.

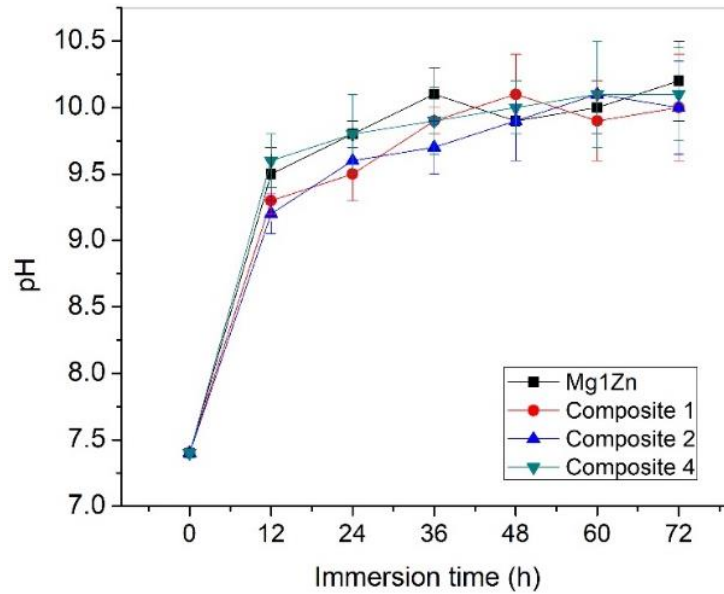


**Figure 6.** Comparison of pH change of the samples for 72 h of immersion time.

Figure 7 shows the photographs of the immersed samples (72 h) after removing the corrosion products. It is visually observed that compared with base alloy, composites have a lower number of pits and regions of surface degradation. Figure 8 compares % of weight loss of the immersed samples. With the increased immersion time for all the samples, weight loss was measured as increased. Composites have shown relatively lower weight loss than base alloys. Particularly, for the composites with 2% and 4% CeO<sub>2</sub>, lower weight loss was recorded. Composite 2 has shown lower degradation compared with all the samples. The improved degradation resistance of the composites is attributed to the stability of the magnesium hydroxide and the deposition of Ca-based mineral phases.

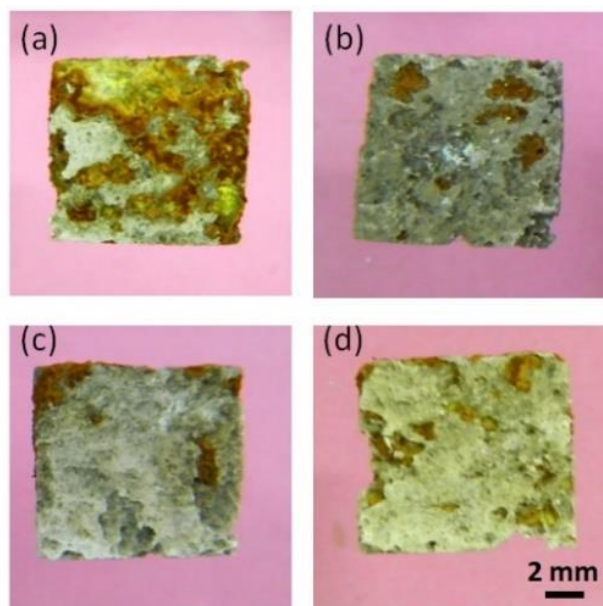


**Figure 7.** Photographs of the immersed samples (72 h) after removing the corrosion products: (a) Mg1Zn; (b) composite 1; (c) composite (2); (d) composite 4.

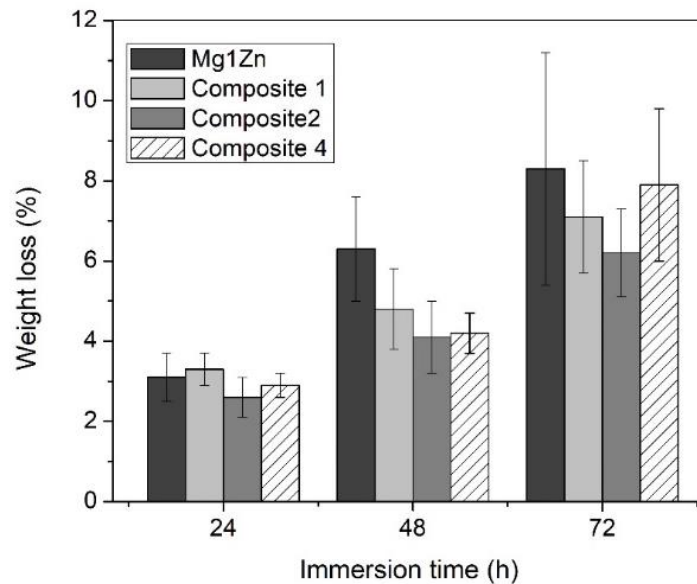


**Figure 8.** Comparison of the % of weight loss of the immersed samples.

It was also noticed that the degradation was increased for composite 4 compared with composite 1 and composite 2 after 72 hours of immersion. Increased CeO<sub>2</sub> content of up to 4% increases galvanic corrosion due to the presence of more reinforcement. On the other hand, more mineral depositions and stabilized magnesium hydroxide decrease the degradation. The combined effects of higher reinforcement resulted in a marginal increment of degradation in the composite 4. From the overall results, 2% composite has shown relatively better degradation resistance. It is well understood that the addition of reinforcements enhances the mechanical performance of the composites. In degradable biomaterial applications, enhanced mechanical properties help sustain the implant's mechanical integrity with the local tissue during the degradation process and reduce the mechanical failure of the implant before the completion of its required life span. Hence, assessing the mechanical performance of developed Mg1Zn-CeO<sub>2</sub> subjected to a corroding environment is crucial and is suggested to be carried out as a future scope of work to understand the efficacy of the produced composite for load-bearing implant usage.

#### 4. Conclusions

Composites of Mg1Zn-CeO<sub>2</sub> with different fractions of CeO<sub>2</sub> (1, 2, and 4%) have been produced by stir casting for degradable implant applications. From the microstructural studies, the decreased grain size was measured for the composites up to  $105 \pm 7.1\mu\text{m}$  with 4% CeO<sub>2</sub> compared with the master alloy ( $165 \pm 12.3\mu\text{m}$ ). XRD analysis of the produced composites confirms the impurity-free phases in the produced composites. From the *in vitro* immersion studies, the stability of the magnesium hydroxide layer was noticed, in addition to more Ca-based mineral deposition on the composites compared with the base alloy, which enhanced the degradation resistance. The reinforcement benefit was observed to be higher for the composites, with 2% and 4%. The XRD analysis also demonstrates the stability of the produced corrosion layer on the composite samples compared with the Mg1Zn alloy. The weight loss measurements indicate the promising role of CeO<sub>2</sub> in decreasing the degradation, as reflected by the lower weight loss at 24, 48, and 72h of immersion. Among all the composites, 2% was optimum with better degradation behavior. Hence, it is concluded that novel Mg1Zn-CeO<sub>2</sub> composites produced by the stir casting route can be viable candidates for manufacturing



temporary implants with enhanced performance. However, the mechanical performance of these composites subjected to mechanical loading needs to be investigated to understand their potential for load-bearing implant applications.

## Funding

This research received no external funding

## Acknowledgments

The authors thank the Centre of Excellence – CoExAMMPC, School of Applied Science and Humanities, Vignan's Foundation for Science, Technology, and Research; Vadllamudi, India, for helping in materials characterization.

## Conflicts of Interest

The authors declare no conflict of interest.

## References

1. Zhang, T.; Wang, W.; Liu, J.; Wang, L.; Tang, Y.; Wang, K. A review on magnesium alloys for biomedical applications. *Front. Bioeng. Biotechnol.* **2022**, *10*, 953344, <http://doi.org/10.3389/fbioe.2022.953344>.
2. He, M.; Chen, L.; Yin, M.; Xu, S.; Liang, Z. Review on magnesium and magnesium-based alloys as biomaterials for bone immobilization. *J. Mater. Res. Technol.* **2023**, *23*, 4396-4419, <https://doi.org/10.1016/j.jmrt.2023.02.037>.
3. Amukarimi, S.; Mozafari, M. Biodegradable Magnesium Biomaterials—Road to the Clinic. *Bioengineering* **2022**, *9*, 107, <https://doi.org/10.3390/bioengineering9030107>.
4. Uppal, G.; Thakur, A.; Chauhan, A.; Bala, S. Magnesium based implants for functional bone tissue regeneration – A review. *J. Magnes. Alloys.* **2022**, *10*, 356-386, <https://doi.org/10.1016/j.jma.2021.08.017>.
5. Guan, H.; Xiao, H.; Ouyang, S.; Tang, A.; Chen, X.; Tan, J.; Feng, B.; She, J.; Zheng, K.; Pan, F. A review of the design, processes, and properties of Mg-based composites. *Nanotechnol. Rev.* **2022**, *11*, 712-730, <https://doi.org/10.1515/ntrev-2022-0043>.
6. Venkateswarlu, B.; Sunil, B.R.; Kumar, R.S. Magnesium based alloys and composites: Revolutionized biodegradable temporary implants and strategies to enhance their performance. *Materialia* **2023**, *27*, 101680, <https://doi.org/10.1016/j.mtla.2023.101680>.
7. Krishnan, R.; Pandiaraj, S.; Muthusamy, S.; Panchal, H.; Alsoofi, M.S.; Ibrahim, A.M.M.; Elsheikh, A. Biodegradable magnesium metal matrix composites for biomedical implants: synthesis, mechanical performance, and corrosion behavior – a review. *J. Mater. Res. Technol.* **2022**, *20*, 650-670, <https://doi.org/10.1016/j.jmrt.2022.06.178>.
8. Yuan, B.; Chen, H.; Zhao, R.; Deng, X.; Chen, G.; Yang, X.; Xiao, Z.; Aurora, A.; Iulia, B.A.; Zhang, K.; Zhu, X.; Iulian, A.V.; Hai, S.; Zhang, X. Construction of a magnesium hydroxide/graphene oxide/hydroxyapatite composite coating on Mg-Ca-Zn-Ag alloy to inhibit bacterial infection and promote bone regeneration. *Bioact. Mater.* **2022**, *18*, 354-367, <http://doi.org/10.1016/j.bioactmat.2022.02.030>.
9. Antoniac, I.; Adam, R.; Biță, A.; Miculescu, M.; Trante, O.; Petrescu, I.M.; Pogărașteanu, M. Comparative Assessment of In Vitro and In Vivo Biodegradation of Mg-1Ca Magnesium Alloys for Orthopedic Applications. *Materials* **2021**, *14*, 84, <https://doi.org/10.3390/ma14010084>.
10. Li, W.; Shen, Y.; Shen, J.; Shen, D.; Liu, X.; Zheng, Y.; Yeung, K.W.K.; Guan, S.; Kulyasova, O.B.; Valiev, R.Z. In vitro and in vivo studies on pure Mg, Mg-1Ca and Mg-2Sr alloys processed by equal channel angular pressing. *Nano Mater. Sci.* **2020**, *2*, 96-108, <https://doi.org/10.1016/j.nanoms.2020.03.004>.
11. Sangeetha, V.J.; Dutta, S.; Moses, J.A.; Anandharamkrishnan, C. Zinc nutrition and human health: Overview and implications. *eFood* **2022**, *3*, e17, <https://doi.org/10.1002/efd2.17>.
12. Neil, W.C.; Forsyth, M.; Howlett, P.C.; Hutchinson, C.R. and Hinton, B.R.W. Corrosion of magnesium alloy ZE41 – The role of microstructural features, *Corros. Sci.* **2009**, *51*, 387-394, <https://doi.org/10.1016/j.corsci.2008.11.005>

13. Okamoto, H.; Subramanian, P. R.; Kacprzak, L. Binary Alloy Phase Diagrams. Massalski, T.B., Eds.; Metals Park, OH: American Society for Metals. **2016**, Volume 3, <https://doi.org/10.31399/asm.hb.v03.a0006247>.
14. Feng, N.; Liu, Y.; Dai, X.; Wang, Y.; Guo, Q.; Li, Q. Advanced applications of cerium oxide based nanozymes in cancer. *RSC Adv.* **2022**, *12*, 1486–1493, <http://doi.org/10.1039/D1RA05407D>.
15. Hosseini, M.; Mozafari, M. Cerium Oxide Nanoparticles: Recent Advances in Tissue Engineering. *Materials* **2020**, *13*, 3072, <http://doi.org/10.3390/ma13143072>.
16. Pansambal, S.; Oza, R.; Borgave, S.; Chauhan, A.; Bardapurkar, P.; Vias, S.; Ghotekar, S. Bioengineered cerium oxide (CeO<sub>2</sub>) nanoparticles and their diverse applications: a review. *Appl. Nanosci.* **2022**, *13*, 6067–6092, <https://doi.org/10.1007/s13204-022-02574-8>.
17. Davan, R.; Prasad, R.G.S.V.; Jakka, V.S.; Aparna, R.S.L.; Phani, A.R.; Jacob, B.; Salins, P.C.; Raju, D.B. Cerium Oxide Nanoparticles Promotes Wound Healing Activity in *In-Vivo* Animal Model. *J. Bionanosci.* **2012**, *6*, 78–83, <https://doi.org/10.1166/jbns.2012.1074>.
18. Legon'kova, O.A.; Ushakova, T.A.; Savchenkova, I.P.; Perova, N.V.; Belova, M.S.; Torkova, A.A.; Baranchikov, A.E.; Ivanova, O.S.; Korotaeva, A.I.; Ivanov, V.K. Experimental Study of the Effects of Nanodispersed Ceria on Wound Repair. *Bull. Exp. Biol. Med.* **2017**, *162*, 395–399, <http://doi.org/10.1007/s10517-017-3624-2>.
19. Ermakov, A.; Popov, A.; Ermakova, O.; Ivanova, O.; Baranchikov, A.; Kamenskikh, K.; Shekunova, T.; Shcherbakov, A.; Popova, N.; Ivanov, V. The first inorganic mitogens: Cerium oxide and cerium fluoride nanoparticles stimulate planarian regeneration *via* neoblastic activation. *Mater. Sci. Eng. C* **2019**, *104*, 109924, <https://doi.org/10.1016/j.msec.2019.109924>.
20. Kalyanaraman, V.; Naveen, S.V.; Mohana, N.; Balaje, R.M.; Navaneethakrishnan, K.R.; Brabu, B.; Murugan, S.S.; Kumaravel, T.S. Biocompatibility studies on cerium oxide nanoparticles—combined study for local effects, systemic toxicity and genotoxicity via implantation route. *Toxicol. Res.* **2019**, *8*, 25–37, <https://doi.org/10.1039/C8TX00248G>.
21. Prefac, G.-A.; Milea, M.-L.; Vadureanu, A.-M.; Muraru, S.; Dobrin, D.-I.; Isopencu, G.-O.; Jinga, S.-I.; Raileanu, M.; Bacalum, M.; Busuioc, C. CeO<sub>2</sub> Containing Thin Films as Bioactive Coatings for Orthopaedic Implants. *Coatings* **2020**, *10*, 642, <http://doi.org/10.3390/coatings10070642>.
22. Shcherbakov, A.B.; Reukov, V.V.; Yakimansky, A.V.; Krasnopeeveva, E.L.; Ivanova, O.S.; Popov, A.L.; Ivanov, V.K. CeO<sub>2</sub> Nanoparticle-Containing Polymers for Biomedical Applications: A Review. *Polymers* **2021**, *13*, 924, <https://doi.org/10.3390/polym13060924>.
23. Kokubo, T.; Takadama, H. How useful is SBF in predicting in vivo bone bioactivity?. *Biomaterials* **2006**, *27*, 2907–2915, <http://doi.org/10.1016/j.biomaterials.2006.01.017>.
24. Ratna Sunil, B.; Sampath Kumar, T.S.; Chakkingal, U.; Nandakumar, V.; Mukesh, D. Nano-hydroxyapatite reinforced AZ31 magnesium alloy by friction stir processing: a solid state processing for biodegradable metal matrix composites. *J. Mater. Sci. Mater. Med.* **2014**, *25*, 975–988, <http://doi.org/10.1007/s10856-013-5127-7>.
25. Wang, Y.; Li, Z.; Wang, Y.; Sun, T.; Ba, Z. Corrosion Resistance of Mg(OH)<sub>2</sub>/Mn(OH)<sub>2</sub> Hydroxide Film on ZK60 Mg Alloy. *Metals* **2022**, *12*, 1760, <https://doi.org/10.3390/met12101760>.
26. Shu, Y.; Peng, F.; Xie, Z.-H.; Yang, Q.; Wu, L.; Xie, J.; Li, M. Well-oriented magnesium hydroxide nanoplatelets coating with high corrosion resistance and osteogenesis on magnesium alloy. *J. Magnes. Alloys.* **2023**, <https://doi.org/10.1016/j.jma.2023.02.002>.
27. Sunil, B.R.; Kumar, A.A.; Sampath Kumar, T.S.; Chakkingal, U. Role of biomineralization on the degradation of fine grained AZ31 magnesium alloy processed by groove pressing. *Mater. Sci. Eng. C.* **2013**, *33*, 1607–1615, <https://doi.org/10.1016/j.msec.2012.12.095>.
28. Zhi, P.; Liu, L.; Chang, J.; Liu, C.; Zhang, Q.; Zhou, J.; Liu, Z.; Fan, Y. Advances in the Study of Magnesium Alloys and Their Use in Bone Implant Material. *Metals* **2022**, *12*, 1500, <https://doi.org/10.3390/met12091500>.
29. Sunil, B.R.; Sampath Kumar, T.S.; Chakkingal, U.; Nandakumar, V.; Doble, M. Friction stir processing of magnesium–nanohydroxyapatite composites with controlled *in vitro* degradation behaviour. *Mater. Sci. Eng. C.* **2014**, *39*, 315–324. <https://doi.org/10.1016/j.msec.2014.03.004>.
30. Sunil, B.R.; Sampath Kumar, T.S.; Chakkingal, U. Bioactive Grain Refined Magnesium by Friction Stir Processing. *Mater. Sci. Forum.* **2012**, *710*, 264–269, <http://doi.org/10.4028/www.scientific.net/MSF.710.264>.

31. Dong, J.; Lin, T.; Shao, H.; Wang, H.; Wang, X.; Song, K.; Li, Q. Advances in degradation behavior of biomedical magnesium alloys: A review. *J. Alloys Comp.* **2022**, *908*, 164600, <https://doi.org/10.1016/j.jallcom.2022.164600>.
32. Zohdy, K.M.; El-Sherif, R.M.; El-Shamy, A.M. Effect of pH fluctuations on the biodegradability of nanocomposite Mg-alloy in simulated bodily fluids. *Chem. Pap.* **2023**, *77*, 1317–1337, <https://doi.org/10.1007/s11696-022-02544-y>.